

# A semi-supervised feature selection method for image inpainting in Fourier transform domain

Yingfu Cai<sup>a</sup>, Xiaoyang Yu<sup>a\*</sup>, Ali Tavakoli<sup>b</sup>

## Abstract

This paper deals with recovering an image some of which Fourier transform coefficients are lost. Based on a semi-supervised feature selection method, we first present a truncated singular value decomposition approach and second present a new minimization algorithm for image inpainting in the Fourier transform domain. The convergence of this algorithm is also proved. Finally, some comparisons of the given methods and some known algorithms are presented to show the efficiency of our approaches.

**Keywords:** Image Inpainting · Fourier transform domain · Semi-supervised selection method  
**Mathematics Subject Classification (2000)** 94A08 · 90C27 · 65T50

## 1. Introduction

Image inpainting is recovering an image or video, part of which observed data is incomplete. The lost data may be related to either intensity of the pixels in an area of the target image or the coefficients of transform domain [2,24].

Transformed domain inpainting practically happens in applications because images are usually formatted, transmitted, and stored in a transform domain. For instance, JPEG standard images are encoded in terms of discrete cosine transform coefficients and JPEG 2000 standard images are

encoded by wavelet transform coefficients, and in magnetic resonance (MR) imaging the acquired data are Fourier transform coefficients [6,7]. When some of the coefficients of the transform domain such as Fourier or wavelet transform are lost, the inverse transform can not naturally construct the original image. In this case, we need to inpaint the images in the transform domain to retrieve the original image as well as possible.

It can be done by using the information of the surrounding areas. Of course, one notes that by the definition of discrete Fourier transform for a 2D image  $I$  of size  $m \times n$ , i.e.,

$$F(s, t) = \sum_{x=0}^{m-1} \sum_{y=0}^{n-1} I(x, y) e^{-2\pi j \left( \frac{sx}{m} + \frac{ty}{n} \right)}, \quad s = 0, \dots, m-1, \quad t = 0, \dots, n-1,$$

the following relation holds:

$$F^H(s, t) = F(m-s, n-t), \quad s = 0, \dots, m-1, \quad t = 0, \dots, n-1,$$

---

*a* The higher educational key laboratory for Measuring & Control Technology and Instrumentation of Heilongjiang province, Harbin University of Science and Technology, Harbin 150080, China  
*b* Mathematics department, University of Mazandaran, Babolsar, Iran  
\*Corresponding Author: Xiaoyang Yu  
Email: [pangyuan39r@126.com](mailto:pangyuan39r@126.com)

---

where  $H$  denotes the conjugate operator. Hence, during the restoration in the Fourier transform domain, it is enough to save only half of the Fourier coefficients. In 2016, Li and Zeng introduced an algorithm called iterative coupled transform domain inpainting (ICTDI) for reconstruction of an image some of which Fourier transform coefficients are lost [18]. It uses two positive parameters to adjust the weight of each term of the given least square minimization problem. Some modifications of Algorithm ICTDI that benefit one more parameter to have more degree of freedom are given in [19] and [20].

In this paper, we used a semi-supervised feature selection method to first approximate the intensities of some pixels that are called auxiliary pixels. Next, a linear system is constituted whose solution is approximated by a truncated singular value decomposition method. Then by a perturbation in the auxiliary points, a minimization problem is presented whose convergence is also proved.

## 2. A semi-supervised feature selection method

In this section, we present an algorithm based on a semi-supervised feature selection method for image inpainting in the Fourier transform domain. The methodology simply can be expressed as follows:

$$F(u, v) = F^H(M - u, N - v), (u, v) \in X \quad (1)$$

where  $X = \{0, 1, \dots, M - 1\} \times \{0, 1, \dots, N - 1\}$ . It is readily seen that there do not exist the conjugate of  $F(u, 0)$  for  $u = 0, 1, \dots, M - 1$  and  $F(0, v)$  for  $v = 0, 1, \dots, N - 1$ . Also, it is clear that we must consider the case that  $F(u, v)$  and  $F(M - u, N - v)$  are lost, simultaneously. In the sequel, we define:

$$\begin{aligned} K &= \{(u, v) \in X \mid F(u, v) \text{ is in access}\}, \\ L &= \{(u, v) \in X \mid F(u, v) \text{ is lost and } uv \neq 0\}, \\ L' &= \{(u, v) \in X \mid F(u, v) \text{ is lost and } uv = 0\}, \\ Y &= \{(x, y) \in X \mid (x, y) \text{ is an auxiliary point}\}. \end{aligned}$$

By definition of the inverse Fourier transform for each  $(x, y) \in Y$  we have:

$$f(x, y) = \frac{1}{MN} \left( \sum_{(u,v) \in K} F(u, v) e^{2\pi j \left( \frac{ux}{M} + \frac{vy}{N} \right)} + \sum_{(u,v) \in L \cup L'} F(u, v) e^{2\pi j \left( \frac{ux}{M} + \frac{vy}{N} \right)} \right), \quad (2)$$

Let  $F(u, v) = G(u, v) + jH(u, v)$  for  $(u, v) \in X$  and also  $\lfloor x \rfloor$  and  $\lceil x \rceil$  denote the largest integer number less than or equal to  $x$  and the smallest integer number bigger than or equal to  $x$ , respectively. We also define the following sets:

$$\begin{aligned} L_1 &= L \cap \left\{ \left\{ 1, 2, \dots, \left\lfloor \frac{M}{2} \right\rfloor \right\} \times \left\{ 1, 2, \dots, \left\lfloor \frac{N}{2} \right\rfloor \right\} \right\} \\ L_2 &= L \cap \left\{ \left\{ 1, 2, \dots, \left\lfloor \frac{M}{2} \right\rfloor \right\} \times \left\{ \left\lceil \frac{N}{2} \right\rceil, \dots, N - 1 \right\} \right\} \end{aligned}$$

First, the inverse Fourier transform of the missing Fourier transform naturally generate an image with fairly high mean square error (MSE). This image is a corrupted image whose contrast depends on the percentage of lost Fourier transform coefficients. However, an image is derived wherewithal the general feature of the original image is some deal identified. Although the exact intensity of each pixel is not clear and it is a stochastic variable, some pixels of the image can be determined by a good approximation. For example, Figure 2 shows the picture of a cameraman by the inverse Fourier transform whose 30 percent of Fourier transform coefficients are missing. It is clear that the intensity of some pixels such as the points on the coat of cameraman should be about zero. This, in turn, contains some pixels that hereafter we call them auxiliary points. By these auxiliary points, one can find a (fairly) good approximation for the intensity level of all pixels. Suppose that the number of auxiliary points and lost Fourier coefficients are the same. In this case, if the auxiliary points are exactly chosen, we can derive the original image precisely whenever the resulted system is accurately solved! In order to formulate this, let  $F$  be the Fourier transform of an  $M \times N$  image  $f$  whose some of the coefficients are missing. Let  $F^H$  be the conjugate of  $F$ . One note that

$$L_3 = L \cap (\{\lfloor \frac{M}{2} \rfloor, \dots, M-1\} \times \{1, 2, \dots, \lfloor \frac{N}{2} \rfloor\})$$

$$L_4 = L \cap (\{\lfloor \frac{M}{2} \rfloor, \dots, M-1\} \times \{\lfloor \frac{N}{2} \rfloor, \dots, N-1\}).$$

Now, requirement (1) and the preceding definitions imply that

$$\sum_{(u,v) \in L_4} F(u, v) e^{2\pi j \left(\frac{ux}{M} + \frac{vy}{N}\right)} = \sum_{(u,v) \in L_1} F^H(u, v) e^{-2\pi j \left(\frac{ux}{M} + \frac{vy}{N}\right)}$$

$$\sum_{(u,v) \in L_3} F(u, v) e^{2\pi j \left(\frac{ux}{M} + \frac{vy}{N}\right)} = \sum_{(u,v) \in L_2} F^H(u, v) e^{-2\pi j \left(\frac{ux}{M} + \frac{vy}{N}\right)}. \quad (3)$$

Therefore,

$$\sum_{(u,v) \in L} F(u, v) e^{2\pi j \left(\frac{ux}{M} + \frac{vy}{N}\right)}$$

$$= \sum_{(u,v) \in L_1} F(u, v) e^{2\pi j \left(\frac{ux}{M} + \frac{vy}{N}\right)} + F^H(u, v) e^{-2\pi j \left(\frac{ux}{M} + \frac{vy}{N}\right)} + \sum_{(u,v) \in L_2} F(u, v) e^{2\pi j \left(\frac{ux}{M} + \frac{vy}{N}\right)} +$$

$$F^H(u, v) e^{-2\pi j \left(\frac{ux}{M} + \frac{vy}{N}\right)}$$

$$= \sum_{(u,v) \in L_1} 2[G(u, v) \cos(2\pi(ux/M + vy/N)) - H(u, v) \sin(2\pi(ux/M + vy/N))] \quad (4)$$

$$+ \sum_{(u,v) \in L_2} 2[G(u, v) \cos(2\pi(ux/M + vy/N)) - H(u, v) \sin(2\pi(ux/M + vy/N))]$$

$$= \sum_{(u,v) \in L_1 \cup L_2} 2 \cos(2\pi(ux/M + vy/N)) G(u, v) - \sum_{(u,v) \in L_1 \cup L_2} 2 \sin(2\pi(ux/M + vy/N)) H(u, v)$$

So,

$$f(x, y) = \frac{1}{MN} \left( \sum_{(u,v) \in K} F(u, v) e^{2\pi j \left(\frac{ux}{M} + \frac{vy}{N}\right)} + \sum_{(u,v) \in L_1 \cup L_2} 2 \cos\left(2\pi \left(\frac{ux}{M} + \frac{vy}{N}\right)\right) G(u, v) \right.$$

$$\left. - \sum_{(u,v) \in L_1 \cup L_2} 2 \sin\left(2\pi \left(\frac{ux}{M} + \frac{vy}{N}\right)\right) H(u, v) \right) \quad (5)$$

Let  $\bar{f}$  be the inverse Fourier transform of the incomplete Fourier transform  $F$ . In other words,  $\bar{f}$  is produced just by  $F(u, v)$  for  $(u, v) \in K$ . Assume that for  $(x, y) \in Y$ ,  $\hat{f}(x, y)$  are the intensity level of auxiliary points. In order to obtain a good reconstruction of  $f(x, y)$  for  $(x, y) \in X \setminus Y$ , we find  $\tilde{F}$  such that for  $(x, y) \in Y$

$$\hat{f}(x, y) = \frac{1}{MN} \left( \sum_{(u,v) \in K} F(u, v) e^{2\pi j \left(\frac{ux}{M} + \frac{vy}{N}\right)} + \sum_{(u,v) \in L_1 \cup L_2} \tilde{F}(u, v) e^{2\pi j \left(\frac{ux}{M} + \frac{vy}{N}\right)} \right)$$

Now, taking

$$\tilde{f}(x, y) = \hat{f}(x, y) - \frac{1}{MN} \sum_{(u,v) \in K} F(u, v) e^{2\pi j \left(\frac{ux}{M} + \frac{vy}{N}\right)}, \quad (x, y) \in Y \quad (6)$$

and  $\tilde{F} \equiv \tilde{G} + j \tilde{H}$  into account, the preceding relations imply

$$\tilde{f}(x, y) = \frac{1}{MN} \left( \sum_{(u,v) \in L'} \tilde{F}(u, v) e^{2\pi j \left(\frac{ux}{M} + \frac{vy}{N}\right)} + \sum_{(u,v) \in L_1 \cup L_2} 2 \cos\left(2\pi \left(\frac{ux}{M} + \frac{vy}{N}\right)\right) \tilde{G}(u, v) \right.$$

$$\left. - \sum_{(u,v) \in L_1 \cup L_2} 2 \sin\left(2\pi \left(\frac{ux}{M} + \frac{vy}{N}\right)\right) \tilde{H}(u, v) \right) \quad (7)$$

The equality (7) can be expressed in a matrix form by

$$\tilde{\mathbf{f}} = S\mathbf{x}$$

where

$$S = \frac{1}{MN} \begin{bmatrix} \tilde{\mathbf{P}} & \tilde{\mathbf{A}} & \tilde{\mathbf{B}} \end{bmatrix} \begin{matrix} (u,v) \in L' \\ (u,v) \in L_1 \cup L_2 \\ (u,v) \in L_1 \cup L_2 \end{matrix}$$

$$\mathbf{x} = \begin{bmatrix} \mathbf{p} \\ \mathbf{g} \\ \mathbf{h} \end{bmatrix} \begin{matrix} (u,v) \in L' \\ (u,v) \in L_1 \cup L_2 \\ (u,v) \in L_1 \cup L_2 \end{matrix} \quad (9)$$

$$\tilde{\mathbf{f}} = \left( \tilde{f}(x, y) \right)_{(x,y) \in \Upsilon} \text{ and}$$

$$\begin{cases} P_{r,p} = e^{2\pi j(ux/M + vy/N)}, & r := (x, y) \in \Upsilon, p := (u, v) \in L', \\ A_{r,s} = 2 \cos(2\pi(ux/M + vy/N)), & r := (x, y) \in \Upsilon, s := (u, v) \in L_1 \cup L_2, \\ B_{r,t} = -2 \sin(2\pi(ux/M + vy/N)), & r := (x, y) \in \Upsilon, t \in L_1 \cup L_2. \end{cases}$$

Therefore,

$$\tilde{F}(u, v) = \begin{cases} \mathbf{p}(u, v), & (u, v) \in L', \\ \mathbf{g}(u, v) + j\mathbf{h}(u, v), & (u, v) \in L_1 \cup L_2. \end{cases}$$

We note that if  $L' = \emptyset$ , then the matrix  $S$  will be real.

### 3. Truncated SVD method

In this section, we present the truncated singular value decomposition to present an approximated solution of (8). Letting  $|\mathbf{a}|$  as the cardinal number of the vector  $\mathbf{a}$ , the size of  $S$  is  $|\Upsilon| \times (|L'| + 2|L_1 \cup L_2|)$ . It is well known that the linear system (8), will have a solution if  $|\Upsilon| \leq (|L'| + 2|L_1 \cup L_2|)$ . Since,  $S$  is a dense matrix and moreover the size of an image and so the size of the Fourier transform coefficients is usually big, therefore, even if a few percentages of

the Fourier transform coefficients are lost, the dimension of the matrix  $S$  would (fairly) be high. This implies that if  $|\Upsilon| = |L'| + 2|L_1 \cup L_2|$  and  $S$  is a non-singular matrix, the direct solving of the system (8) will usually be impossible. Under condition  $|\Upsilon| \leq (|L'| + 2|L_1 \cup L_2|)$ , to find an approximated solution of (8) one can use the truncated singular value decomposition (TSVD) method. To this end, it is recalled that the matrix  $S$  can be factored as

$$S = U\Sigma V^H, \quad (10)$$

where  $U$  is an  $|\Upsilon| \times |\Upsilon|$  unitary matrix,  $\Sigma$  is an  $|\Upsilon| \times (|L'| + 2|L_1 \cup L_2|)$  diagonal matrix,  $V$  is an  $(|L'| + 2|L_1 \cup L_2|) \times (|L'| + 2|L_1 \cup L_2|)$  unitary matrix [17].

Let  $\sigma_1^2, \sigma_2^2, \dots, \sigma_n^2$  be the singular values of  $S$  such that

$$\sigma_1^2 \leq \sigma_2^2 \leq \dots \leq \sigma_n^2$$

and

$$\begin{cases} \sigma_i^2 > 0, & i = 1, \dots, r \\ \sigma_i^2 = 0, & i = r + 1, \dots, n. \end{cases} \quad (11)$$

The pseudo-inverse of



where  $\lambda$  is a positive constant. It is readily seen that the closed form solution of (17), then it satisfies the following equation:

$$\begin{bmatrix} (1 + \lambda)I & -S \\ -S^H & S^H S \end{bmatrix} \begin{bmatrix} \mathbf{f}^* \\ \mathbf{x} \end{bmatrix} = \begin{bmatrix} \lambda \hat{\mathbf{f}} + \bar{\mathbf{F}} \\ -S^H \bar{\mathbf{F}} \end{bmatrix}, \quad (18)$$

where  $I$  is an identity matrix of size  $|Y| \times |Y|$ . If  $S^H S$  is non-singular, then the saddle point system (18) has a unique solution, because  $(1 + \lambda)I$  is a positive definite matrix,  $S$  is a full rank matrix and  $S^H S$  is a positive definite matrix (see [1] Section 3.1). However, since  $S^H S$  is not always one to one, in general, (18) is an ill-posed system. Hence, the given system can be approximately solved by some appropriate pre-conditioners [1].

One way to overcome the ill-posedness is to add a regularization term to the energy, hence, a solvable method can be thought of as

$$\min_{\mathbf{f}^*, \mathbf{x}} \|\Phi \mathbf{f}^*\|_p + \frac{\mu}{2} \|\mathbf{f}^* - \bar{\mathbf{F}} - S\mathbf{x}\|_2^2 + \frac{\lambda}{2} \|\mathbf{f}^* - \hat{\mathbf{f}}\|_2^2 \quad (19)$$

where  $\Phi \in R^{Y \times Y}$  is a given transform matrix corresponding to some regularization operators,  $\mu$  is a constant positive regularization parameter and  $p = 0, 1$ . The first term is a smoothing term and there are many choices for  $\Phi$  such as gradient operator, wavelet transform and framelet transform.

By using the variable splitting technique and quadratic penalty method, the problem (19) is rewritten into the following equivalent formulation [18]:

$$\min_{\mathbf{d}, \mathbf{f}^*, \mathbf{x}} E(\mathbf{d}, \mathbf{f}^*, \mathbf{x}) = \|\mathbf{d}\|_p + \frac{\eta}{2} \|\Phi \mathbf{f}^* - \mathbf{d}\|_2^2 + \frac{\mu}{2} \|\mathbf{f}^* - \bar{\mathbf{F}} - S\mathbf{x}\|_2^2 + \frac{\lambda}{2} \|\mathbf{f}^* - \hat{\mathbf{f}}\|_2^2 \quad (20)$$

#### The algorithm

The approximated model (20) can be solved by alternating minimization method as follows:

**Solving  $\mathbf{d}$ :** By setting  $\tau := 1/\eta$  and fixing  $\mathbf{f}^*$  and  $\mathbf{x}$ , the sub-problem for  $\mathbf{d}$  reads:

$$\min_{\mathbf{d}} \|\mathbf{d}\|_p + \frac{\eta}{2} \|\Phi \mathbf{f}^* - \mathbf{d}\|_2^2. \quad (21)$$

In the case of  $p = 0$  [4,18], the sub-problem (21) is solved by hard shrinkage, i.e.

$$\mathbf{d} = \begin{cases} \mathbf{0}, & \text{if } |\Phi \mathbf{f}^* - \mathbf{d}| \leq \sqrt{2\tau}, \\ \Phi \mathbf{f}^*, & \text{otherwise.} \end{cases}$$

When  $p = 1$  [13,18], it is solved by soft shrinkage, that is,

$$\mathbf{d} = \max \{ |\Phi \mathbf{f}^*| - \tau, 0 \} \text{sgn}(\Phi \mathbf{f}^*),$$

where the sign function is defined as

$$\text{sgn}(x) = \begin{cases} 1, & x > 0, \\ 0, & x = 0, \\ -1, & x < 0. \end{cases}$$

**Solving  $\mathbf{f}^*$ :** Now, fixing  $\mathbf{d}$  and  $\mathbf{x}$ , the sub-problem for  $\mathbf{f}^*$  reads

$$\min_{\mathbf{f}^*} \frac{1}{2} \|\Phi \mathbf{f}^* - \mathbf{d}\|_2^2 + \frac{\alpha_1}{2} \|\mathbf{f}^* - \bar{\mathbf{F}} - S\mathbf{x}\|_2^2 + \frac{\alpha_2}{2} \|\mathbf{f}^* - \hat{\mathbf{f}}\|_2^2 \quad (22)$$

where  $\alpha_1 = \frac{\mu}{\eta}$  and  $\alpha_2 = \frac{\lambda}{\eta}$ . The closed form solution for  $\mathbf{f}^*$  is as follows:

$$\mathbf{f}^* = (\Phi^H \Phi + (\alpha_1 + \alpha_2)I)^{-1} (\Phi^H \mathbf{d} + \alpha_1(\bar{\mathbf{F}} + S\mathbf{x}) + \alpha_2 \hat{\mathbf{f}}). \quad (23)$$

Finally, the sub-problem for  $\mathbf{x}$  reads:

$$\min_{\mathbf{x}} \|\mathbf{f}^* - \bar{\mathbf{F}} - S\mathbf{x}\|_2^2. \quad (24)$$

The closed form solution for  $\mathbf{x}$  is as follows:

$$\mathbf{x} = (S^H S)^{-1} [S^H (\mathbf{f}^* - \bar{\mathbf{F}})]. \quad (25)$$

In the algorithm FISVD, we replaced the matrix  $S$  by the truncated SVD given in the previous section. So, taking  $S = U\Sigma V^H$  implies that  $(S^H S)^{-1} S^H = V \Sigma'^+ U^H$

*Remark 1* The initial values  $\mathbf{f}^{*(0)}$  and  $\mathbf{x}^{(0)}$  are given by  $\bar{\mathbf{f}} = (\bar{f}(x, y))$  and (16), respectively.

*Remark 2* In order to get rid of the inversion of  $\Phi^H \Phi + (\alpha_1 + \alpha_2)I$ , it can be approximated by  $(1 + \alpha_1 + \alpha_2)I$ .

---

#### Algorithm 1 FISVD

---

Initialization:  $\alpha_1, \alpha_2, \tau, \hat{\mathbf{f}}, \mathbf{f}^{*(0)}, \bar{\mathbf{F}}, \mathbf{x}^{(0)}$ ;

For  $k = 0, 1, 2, \dots$  repeat until stopping criterion is reached

$\mathbf{d}^{(k+1)} = \text{shrink}_p(\Phi \mathbf{f}^{*(k)}, \tau)$ ;

$\mathbf{f}^{*(k+1)} = (\Phi^H \Phi + (\alpha_1 + \alpha_2)I)^{-1} [\Phi^H \mathbf{d}^{(k)} + \alpha_1(\bar{\mathbf{F}} + U\Sigma V^H \mathbf{x}^{(k)}) + \alpha_2 \hat{\mathbf{f}}]$ ;

Output:  $\mathbf{x}^{(k+1)} = V \Sigma'^+ U^H (\mathbf{f}^{*(k+1)} - \bar{\mathbf{F}})$ .

---

### 5. Convergence analysis

In this section, we prove that for  $\tau > 0$  and appropriate selections of  $\alpha_1$  and  $\alpha_2$ , the Algorithm FISVD is convergent. Before that, we need the following lemma:

**Lemma 1** *The largest singular value of the coefficient matrix  $S$  is  $\geq 1$ .*

*Proof* Let  $\rho(A) := \max\{|\lambda| : \lambda \text{ is an eigenvalue of } A\}$ . Since  $S^H S$  is a Hermitian matrix, one can write:

$$\rho(S^H S) = \max_{\mathbf{z} \neq 0} \frac{\mathbf{z}^H S^H S \mathbf{z}}{\mathbf{z}^H \mathbf{z}} = \max_{\mathbf{z} \neq 0} \frac{\|S\mathbf{z}\|_2^2}{\|\mathbf{z}\|_2^2}. \quad (26)$$

It is enough to show that for some nonzero  $\mathbf{z}$ ,  $\frac{\|S\mathbf{z}\|_2}{\|\mathbf{z}\|_2} \geq 1$ . For this sake, we consider two cases:

Case 1:  $L' \neq \emptyset$ .

By (9), there exist  $r := (x, y) \in Y$  and  $p := (u, v) \in L'$  such that  $Pr, p \neq 0$ . Take  $\mathbf{z} = (0, 0, \dots, 0, 1, 0, \dots, 0)^T$  where 1 is located in the  $p$ -th column. This selection implies that  $\frac{\|S\mathbf{z}\|_2}{\|\mathbf{z}\|_2} \geq 1$ .

Case 2:  $L' = \emptyset$ .

Again, by (9), there exist  $r := (x, y) \in Y$  and  $s := (u, v) \in L_1 \cup L_2$  such that  $A_{rs} B_{rt} \neq 0$ , where  $t = |L_1 \cup L_2| + s$ . Take  $\mathbf{z} = (0, 0, \dots, 0, z_s, 0, \dots, 0, z_t, 0, \dots, 0)^T$  in which  $z_s^2 = z_t^2 = 1$ .

Let  $S(r, :)$  denotes the  $r$ -th row of  $S$ . So,

$$S(r, :)\mathbf{z} = 2(z_s \cos(a) - z_t \sin(a)),$$

where  $a = 2\pi(ux/M + vy/N)$ . Since

$$(z_s \cos(a) - z_t \sin(a))^2 = 1 - z_s z_t \sin(2a),$$

one can define:

$$z_s z_t = \begin{cases} 1, & \sin(2a) \leq 0 \\ -1, & \sin(2a) > 0. \end{cases}$$

This implies that  $|S(r, :)\mathbf{z}| \geq 2$  and so  $\frac{\|S\mathbf{z}\|_2}{\|\mathbf{z}\|_2} \geq 1$ .  $\square$

Now, assume that  $p = 1$ . For any vector  $\mathbf{a} \in \mathcal{C}^N$ , we think of the operator  $S_1$  as a soft shrinkage operator and assume that  $S_2$  denotes the operator  $V \Sigma'^+ U^H$ . The Algorithm FISVD can be simplified as follows:

$$\begin{cases} \mathbf{d}^{(k+1)} = S_1(\Phi \mathbf{f}^{*(k)}); \\ \mathbf{f}^{*(k+1)} = \Gamma^{-1} [\Phi^H \mathbf{d}^{(k)} + \alpha_1 U \Sigma V^H \mathbf{x}^{(k)} + \theta]; \\ \mathbf{x}^{(k+1)} = S_2(\mathbf{f}^{*(k+1)} - \bar{\mathbf{F}}), \end{cases} \quad (27)$$

where  $\Gamma = \Phi^H \Phi + (\alpha_1 + \alpha_2)I$  and  $\theta = \alpha_1 \bar{\mathbf{F}} + \alpha_2 \mathbf{f}$ . We define:

$$\begin{cases} h_1(\mathbf{d}, \mathbf{x}) = \Phi \Gamma^{-1} [\Phi^H \mathbf{d} + \alpha_1 U \Sigma V^H \mathbf{x} + \Theta], \\ h_2(\mathbf{d}, \mathbf{x}) = V \Sigma' + U^H \Gamma^{-1} [\Phi^H \mathbf{d} + \alpha_1 U \Sigma V^H \mathbf{x}] + V \Sigma' + U^H (\Gamma^{-1} \Theta - \bar{\mathbf{F}}), \end{cases}$$

Now, one can rewrite (27) as follows:

$$\begin{cases} \mathbf{d}^{(k+1)} = \mathcal{S}_1 o h_1(\mathbf{d}^{(k)}, \mathbf{x}^{(k)}); \\ \mathbf{f}^{*(k+1)} = \Gamma^{-1} [\Phi^H \mathbf{d}^{(k)} + \alpha_1 U \Sigma V^H \mathbf{x}^{(k)} + \Theta]; \\ \mathbf{x}^{(k+1)} = \mathcal{S}_2 o h_2(\mathbf{d}^{(k)}, \mathbf{x}^{(k)}). \end{cases}$$

We assume that  $n(\Phi) \cap n(S) = \emptyset$  where  $n(A)$  denotes the null space of  $A$ . This implies that the function  $E(\mathbf{d}, \mathbf{f}^*, \mathbf{x})$  in (20) is coercive, that is,  $E(\mathbf{d}, \mathbf{f}^*, \mathbf{x}) \rightarrow \infty$  as  $\|(\mathbf{d}, \mathbf{f}^*, \mathbf{x})\| \rightarrow \infty$ . Moreover,  $E(\mathbf{d}, \mathbf{f}^*, \mathbf{x})$  is convex and bounded from below. Therefore,  $E(\mathbf{d}, \mathbf{f}^*, \mathbf{x})$  has at least one minimizer pair  $(\bar{\mathbf{d}}, \bar{\mathbf{f}}^*, \bar{\mathbf{x}})$  which satisfies the following equations [3]

$$\begin{cases} \bar{\mathbf{d}} = \mathcal{S}_1 o h_1(\bar{\mathbf{d}}, \bar{\mathbf{x}}); \\ \bar{\mathbf{f}}^* = \Gamma^{-1} [\Phi^H \bar{\mathbf{d}} + \alpha_1 U \Sigma V^H \bar{\mathbf{x}} + \Theta]; \\ \bar{\mathbf{x}} = \mathcal{S}_2 o h_2(\bar{\mathbf{d}}, \bar{\mathbf{x}}). \end{cases} \quad (28)$$

The first and third equations of (28) imply that  $(\bar{\mathbf{d}}, \bar{\mathbf{x}})^T$  is a fixed point of  $S o h = (\mathcal{S}_1 o h_1, \mathcal{S}_2 o h_2)$  [15]. Now, the convergence analysis of the given algorithm can be established based on the properties of non-expansiveness of soft shrinkage operator  $\mathcal{S}_1, \mathcal{S}_2$  and  $h$ . The non-expansiveness of  $\mathcal{S}_1$  has been proved in [21,23]. The operator  $\mathcal{S}_2$  is non-expansiveness, because the selection of  $\epsilon = 1$  in (15) implies that

$$\|V \Sigma' + U^H\|_2 \leq \max_{1 \leq i \leq r} \sigma_i^{-1} \leq 1.$$

One note that Lemma 1 concludes that the selection of  $\epsilon = 1$  makes nonzero the matrix  $\Sigma'$ . Let  $\rho(Q)$  denotes the largest absolute eigenvalue of the matrix

$Q$ . By choosing  $N_1 = (\Phi, V \Sigma' + U^H)$  and  $N_2 = (\Phi^H, \alpha_1 U \Sigma V^H)$ , we have:

$$\begin{aligned} \|h(\mathbf{d}, \mathbf{x}) - h(\bar{\mathbf{d}}, \bar{\mathbf{x}})\|_2 &= \left\| \begin{bmatrix} \Phi \Gamma^{-1} \Phi^H & \alpha_1 \Phi \Gamma^{-1} U \Sigma V^H \\ V \Sigma' + U^H \Gamma^{-1} \Phi^H & \alpha_1 V \Sigma' + U^H \Gamma^{-1} U \Sigma V^H \end{bmatrix} \begin{bmatrix} \mathbf{d} - \bar{\mathbf{d}} \\ \mathbf{x} - \bar{\mathbf{x}} \end{bmatrix} \right\|_2 \\ &\leq \|N_1^H \Gamma^{-1} N_2\|_2 \left\| \begin{bmatrix} \mathbf{d} - \bar{\mathbf{d}} \\ \mathbf{x} - \bar{\mathbf{x}} \end{bmatrix} \right\|_2 \\ &\leq \|N_1\|_2 \|\Gamma^{-1}\|_2 \|N_2\|_2 \left\| \begin{bmatrix} \mathbf{d} - \bar{\mathbf{d}} \\ \mathbf{x} - \bar{\mathbf{x}} \end{bmatrix} \right\|_2 \\ &\leq \|N_1\|_2 \|N_2\|_2 \rho(\Gamma^{-1}) \left\| \begin{bmatrix} \mathbf{d} - \bar{\mathbf{d}} \\ \mathbf{x} - \bar{\mathbf{x}} \end{bmatrix} \right\|_2 \\ &\leq \left\| \begin{bmatrix} \mathbf{d} - \bar{\mathbf{d}} \\ \mathbf{x} - \bar{\mathbf{x}} \end{bmatrix} \right\|_2 \end{aligned}$$

The last inequality is readily seen for an enough large value of  $\alpha_2$ , because

$\Gamma$  is a positive definite matrix and  $\rho(\Gamma^{-1}) \leq \frac{1}{\alpha_1 + \alpha_2}$ . Now, based on the non-expansiveness of the

operators  $S$  and  $h$ , the following theorem is proved by a similar argument given in Theorem 3.4 [23] that we have removed it:

**Theorem 1** For any fixed parameters  $\tau > 0$  and suitable selection of  $\alpha_1 > 0$  and  $\alpha_2 > 0$ , the sequence  $\{(\mathbf{d}^k, \mathbf{x}^k, \mathbf{f}^{*(k)})\}$  generated by Algorithm FISVD converges to a solution  $(\bar{\mathbf{d}}, \bar{\mathbf{x}}, \bar{\mathbf{f}}^*)$  of problem (20).





Fig. 1 Test images.

## 6. Numerical results

In this section, we apply the Algorithm FISVD and truncated SVD method on several standard test images in which some coefficients are missing in their Fourier transform domain. Also, these methods are compared with the Algorithm ICTDI and IFTDI given in [18] and [19], respectively. To this

end, we consider three test images called "Cameraman", "Slope", and "Barbara" (see Figure 1). The Slope image contains smooth areas along with sharp edges. The Cameraman image has both large spikes and some fine structures. The image of Barbara contains a few different patterns, e.g. the scarf or the chair.

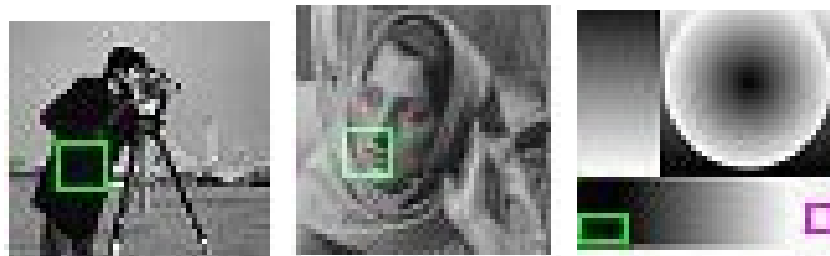


Fig. 2 The auxiliary points are inside of the rectangles.



Fig. 3 Performance of Algorithm FISVD for Cameraman in different iterations: (a) 1st iteration, (b) 45-th iteration, (c) 93-th (last) iteration.

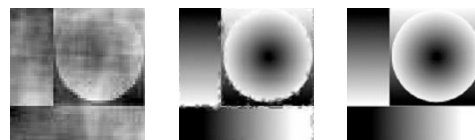


Fig. 4 Performance of Algorithm FISVD for Slope in different iterations: (a) 1st iteration, (b) 40-th iteration, (c) 80-th (last) iteration.

The Standard Peak Signal to Noise Ratio (PSNR) is employed to measure the quantify of inpainting performance [14,10]:

$$PSNR = 10 \log_{10} \left( \frac{255^2}{\|\mathbf{f} - \mathbf{f}^*\|_2} \right) (dB),$$

where  $\mathbf{f}$  is the original image and  $\mathbf{f}^*$  is the reconstructed image (output of the algorithm).

This relation shows that the larger PSNR, the better performance [5]. The stop criterion can be thought of as  $\|\mathbf{f}_*^{(k+1)} - \mathbf{f}_*^{(k)}\| < \varepsilon$  where  $\varepsilon$  is an acceptable tolerance value. Here, we

computed the stopping criterion for Algorithms FISVD, ICTDI and IFTD based on the relative error (ReErr) between the successive iteration of the restored images satisfying the following inequality [18,25]

$$ReErr = \frac{\|\mathbf{f}^{*(k+1)} - \mathbf{f}^{*(k)}\|_2}{\|\mathbf{f}^{*(k+1)}\|_2} < 10^{-5}.$$

In all examples, we consider  $\Phi := \nabla$ , i.e., a gradient operator. As we explained before, the auxiliary points are selected based on our conjecture of the intensity of the original image in some areas. The inside of rectangles

in Figure 2 are considered as auxiliary points of Cameraman, Barbara and Slope, respectively.



**Fig. 5** Performance of Algorithm FISVD for Barbara in different iterations: (a) 1st iteration, (b) 85-th iteration, (c) 172-th (last) iteration.

**Table 1** Comparison of the algorithms for Cameraman

| Method | Iteration | CPU(sec.) | PSNR |
|--------|-----------|-----------|------|
| IFTD   | 80        | 12        | 36   |
| ICTDI  | 79        | 8         | 30   |
| FISVD  | 93        | 15        | 42   |
| TSVD   | -         | -         | 40   |

**Table 2** Comparison of the algorithms for Slope

| Method | Iteration | CPU(sec.) | PSNR |
|--------|-----------|-----------|------|
| ICTDI  | 90        | 8         | 32   |
| IFTD   | 87        | 14        | 35   |
| FISVD  | 80        | 12        | 41   |
| TSVD   | -         | -         | 41   |

**Table 3** Comparison of the algorithms for Barbara

| Method | Iteration | CPU(sec.) | PSNR  |
|--------|-----------|-----------|-------|
| ICTDI  | 115       | 34.91     | 24.01 |
| IFTD   | 137       | 44.50     | 24.26 |
| FISVD  | 172       | 53        | 39    |
| TSVD   | -         | -         | 38    |

For Cameraman,  $\hat{f} \equiv 0.04$  is taken. For Slope image,  $\hat{f} \equiv 0.1$  for the bottom right hand rectangle and  $\hat{f} \equiv 0.9$  for the bottom left hand rectangle are taken. The main problem is related to Barbara image that is hard to find a good approximation of auxiliary points. Hence, the intensity of auxiliary points in Barbara is considered as  $\hat{f} + 0.05$ .

Tables 1, 2 and 3 show comparisons between the Algorithms FISVD, TSVD, ICTDI

[18] and IFTD [19] due to the reconstruction of the Cameraman, Slope and Barbara, respectively. For implementing the Algorithm FISVD, we considered  $\tau = 0.001$  for all three images. For Cameraman and Slope,  $\alpha_1 = 10$  and  $\alpha_2 = 20$  and for Barbara,  $\alpha_1 = \alpha_2 = 100$  are taken. Moreover, for truncated SVD method,  $\epsilon = 1$  is taken. The comparisons show that the algorithm FISV and TSVD method reconstruct the images better than ICTDI and IFTD

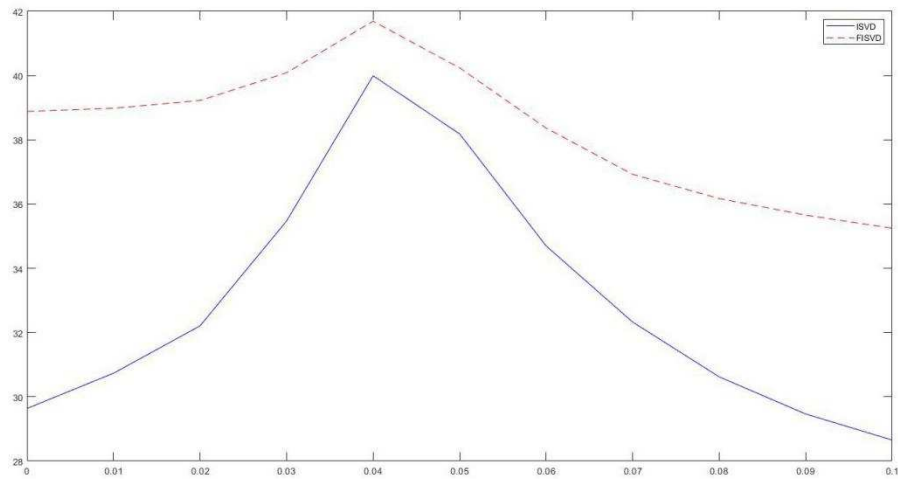


Fig. 6 The PSNR values of FISVD and TSVD algorithms for Cameraman with different auxiliary points.

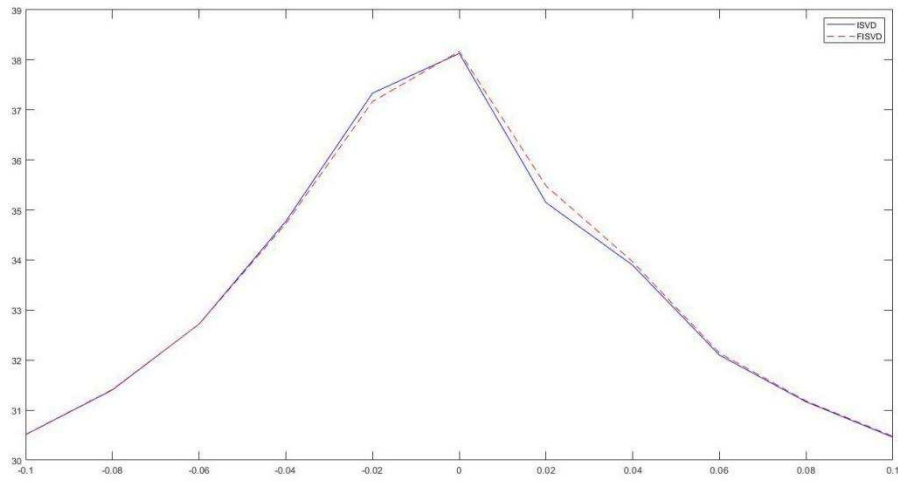
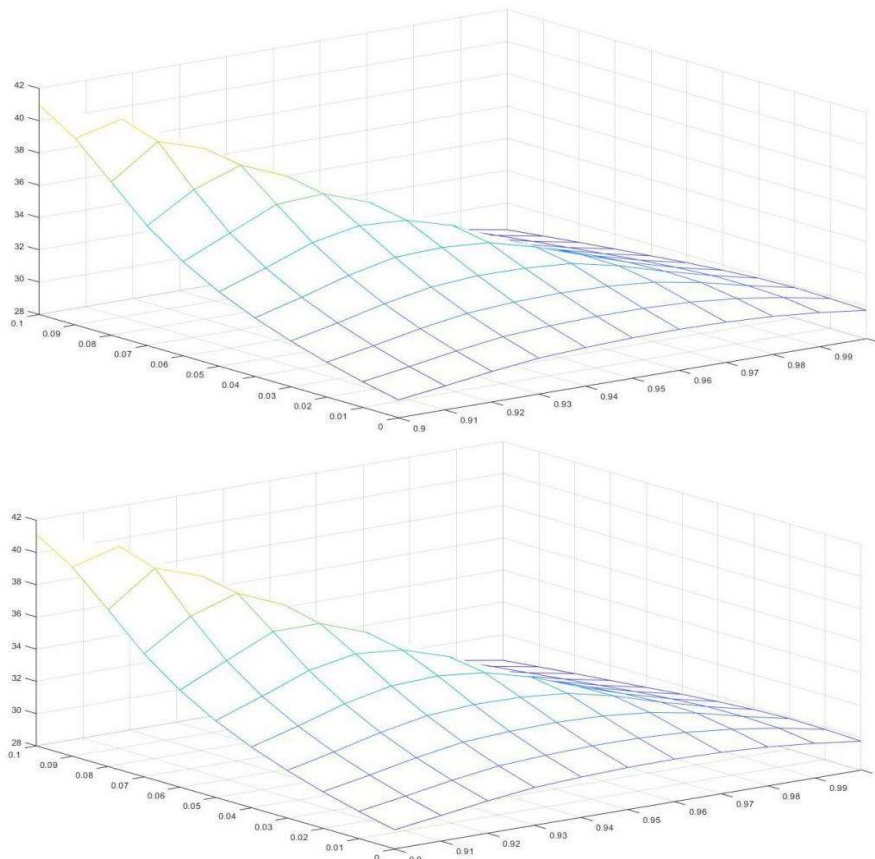


Fig. 7 The PSNR values of FISVD and TSVD algorithms for Barbara with different auxiliary points.



**Fig. 8** The PSNR values of FISVD (bottom) and TSVD (top) algorithms for Slope with different auxiliary points.

All experiments were performed in MATLAB R2018a running on a Sony desktop with Intel Core i5 CPU at 2.40 GHz and 4 GB of memory.

### 7. Conclusion

In this paper, we presented a semi-supervised feature selection method for inpainting an image in the Fourier transform domain. We have used a truncated singular value decomposition to present the algorithm. The experimental results show the efficiency of the proposed algorithm.

### References

- M. Benzi, G. H. Golub and J. Liesen, Numerical solution of saddle point problems, *Acta numerica*, 14 (2005), 1–137.
- M. Bertalmio, G. Sapiro, V. Caselles and C. Ballester, Image inpainting, in *Proceedings of the 27th Annual Conference on Computer Graphics and Interactive Techniques*, ACM Press/Addison-Wesley, Reading, MA, (2000), 417-424.
- D. P. Bertsekas, A. Nedi, A. E. Ozdaglar, *Convex Analysis and Optimization*, Athena Scientific, Belmont, MA, 2003.
- K. Bredies and D. A. Lorenz, Iterated hard shrinkage for minimization problems with sparsity constraints, *SIAM J. Sci. Comput.*, 30 (2008), 657-683.
- T. F. Chan, J. Shen and H. M. Zhou, Total variation wavelet inpainting, *J. Math. Imaging Vis.*, 25 (2006), 107-125.
- R. H. Chan, J. Yang and X. Yuan, Alternating direction method for image inpainting in wavelet domains, *SIAM J. Imaging Sci.*, 4 (2011), 807-826.
- Y. Chen, W. Hager, F. Huang, D. Phan, X. Ye and W. Yin, Fast algorithms for image reconstruction with application to partially parallel MR imaging, *SIAM J. Imaging Sci.*, 5 (2012), 90-118.
- Y. Chen, G. Lan, and Y. Ouyang, Optimal primal-dual methods for a class of saddle point problems, *SIAM J. Optim.*, 24 (2014), pp. 1779-1814.
- E. Corman and X. Yuan, A generalized proximal point algorithm and its convergence rate, *SIAM J. Optim.*, 24 (2014), pp. 1614-1638.

- K. Dabov, A. Foi, V. Katkovnik, and K. Egiazarian, Image denoising by sparse 3D transform-domain collaborative filtering, *IEEE Trans. Image Process.*, 16 (2007), pp. 2080-2095.
- Y. Dong, M. Hintermuller, and M. Neri, An efficient primal-dual method for  $\ell_1$  tv image restoration, *SIAM J. Imaging Sci.*, 2 (2009), pp. 1168-1189.
- R. C. Gonzalez and R. E. Woods, *Digital Image Processing*, Third Edition, Prentice Hall, New Jersey, 2007.
- T. Goldstein and S. Osher, The split Bregman method for  $\ell_1$ -regularized problems, *SIAM J. Imaging Sci.*, 2 (2009), 323-343.
- W. Guo, J. Qin, and W. Yin, A new detail-preserving regularization scheme, *SIAM J. Imaging Sci.*, 7 (2014), pp. 1309–1334.
- T. Hale, W. Yin, and Y. Zhang, Fixed-point continuation for  $\ell_1$ -minimization: Methodology and convergence, *SIAM J. Optim.*, 19 (2008), pp. 1107-1130.
- B. He, Y. You, and X. Yuan, On the convergence of primal-dual hybrid gradient algorithm, *SIAM J. Imaging Sci.*, 7 (2014), pp. 2526-2537.
- D. Kincaid and W. Cheney (1990), *Numerical Analysis*, Brooks/ Cole Publishing Company.
- F. Li and T. Zeng, A new algorithm framework for image inpainting in transform domain, *SIAM J. Imaging Sci.*, 9 (2016), 24-51.
- P. Mousavi and A. Tavakoli, A new algorithm for image inpainting in Fourier transform domain, *Comp. Appl. Math.*, (2019) 38: 22. <https://doi.org/10.1007/s40314-019-0761-4>.
- A. Tavakoli, P. Mousavi and F. Zarmehi, Modified algorithms for image inpainting in Fourier transform domain, *Comp. Appl. Math.*, 37(4)(2), 2019
- F. Li and T. Zeng, A universal variational framework for sparsity based image inpainting, *IEEE Trans. Image Process.*, 23 (2014), 4242-4254.
- S. Setzer, Operator splittings, bregman methods and frame shrinkage in image processing, *Int. J. Comput. Vis.*, 92 (2011), pp. 265-280.
- Y. Wang, J. Yang, W. Yin and Y. Zhang, A new alternating minimization algorithm for total variation image reconstruction, *SIAM J. Imaging Sci.*, 1 (2008), 248-272.
- X. Ye and H. Zhou, Fast total variation wavelet inpainting via approximated primal-dual hybrid gradient algorithm, *Inverse Probl. Imaging*, 7 (2013), 1031-1050.
- X. L. Zhao, W. Wang, T. Y. Zeng, T. Z. Huang, and M. K. Ng, Total variation structured total least squares method for image restoration, *SIAM J. Sci. Comput.*, 35 (2013), pp. B1304-B1320.